# BORATE GLASSES, CRYSTALS & MELTS

Edited by:

Adrian C. WRIGHT, Steven A. FELLER and Alex C. HANNON


**The Society of Glass Technology**
**Sheffield,1997**

# A STRUCTURAL STUDY OF SILVER BORATE GLASSES BY INFRARED REFLECTANCE AND RAMAN SPECTROSCOPIES

John A. KAPOUTSIS, Efstratios I. KAMITSOS & Georgios D. CHRYSSIKOS
*Theoretical and Physical Chemistry Institute, NHRF, 48, Vass. Constantinou Ave., 116 35 Athens, GREECE*

A vibrational spectroscopic study of $xAg_2O.(1-x)B_2O_3$ glasses has been performed to investigate the short- and medium-range structure and the nature of Ag–O bonding as a function of $Ag_2O$ content. The results indicate that the effect of silver oxide on the short-range structure is similar to that of alkali metal oxides, and in particular $Li_2O$. The rate of conversion of $B\varnothing_3$ triangles into $B\varnothing_4^-$ tetrahedra ($\varnothing$=bridging oxygen atom) follows the x/(1–x) law up to *ca* x=0·25, and then it deviates at higher values of x because of the formation of non-bridging oxygen-containing $B\varnothing_2O^-$ triangles. Boroxol rings and other borate arrangements such as, penta-, tri- and di-borate groups, were also identified in Ag-borate glasses with increasing $Ag_2O$ content. The analysis of the far infrared spectra suggests an inhomogeneous distribution of $Ag^+$ ions in the glass matrix. Silver ions in Ag-poor regions behave as pseudo-alkalis and their interactions with the network sites are predominantly ionic, while ions occupying sites in the Ag-rich regions are characterised by a considerable degree of covalency in the Ag–O bonding.

## 1. INTRODUCTION

Borate glasses have attracted the interest of numerous investigators during the last thirty years. Considerable effort has been directed towards the elucidation of glass structure and its dependence on the content and type of alkali metal oxide, $M_2O$. It is well demonstrated that addition of $M_2O$ to $B_2O_3$ causes the gradual change of boron coordination number from three to four, and the formation of non-bridging oxygen atoms at higher modification levels [1-3]. The nature and relative abundance of the various borate arrangements depend strongly on the type of alkali cation [4-6]. It is believed that Ag ions in borate glasses play a role similar to that of the alkalis. Indeed, the results of previous studies have shown that the short-range order of Ag-borate glasses resembles that of alkali borates of the same metal oxide content [7-13].

Interest in silver-borate glasses, $xAg_2O.(1-x)B_2O_3$, has been renewed lately because such compositions can yield superionic glassy conductors after doping with silver halide salts [14] . Kamiya et al [15] proposed on the basis of

their X-ray diffraction study that the enhanced ionic conductivity of Ag-borate glasses originates from a clustering of $Ag^+$ ions, which results in shortening of the jump distance required for the migration of $Ag^+$ charge carriers. Recent molecular dynamics (MD) simulations of the structure of Ag-borates by Abramo et al [16,17] showed that the distribution pattern of silver ions is very sensitive to the choice of silver radius; a small radius (0·63 Å) leads to clustering of $Ag^+$ ions, while the use of a larger radius (1·1 Å) in the simulation process favours their homogeneous distribution.

Besides their high ionic conductivity, silver borate glasses exhibit interesting nonlinear optical properties. It was found recently that the third-order susceptibility, $\chi^{(3)}$, of Ag-borates is much higher than that of Cs-borates, even though $Cs^+$ ions have a larger polarizability than $Ag^+$ ions [18]. To explain such differences it was proposed that the Ag–O bond has considerable covalency as compared to the Cs–O bond which is ionic [18].

In view of this current interest in silver borate glasses, we present in this paper a systematic study of the $xAg_2O.(1-x)B_2O_3$ ($0 \leq x \leq 0{\cdot}33$) system by infrared reflectance and Raman spectroscopic techniques. The purpose of the work is to investigate the effect of $Ag_2O$ on the glass structure and the distribution of $Ag^+$ ions, as well as on the nature of the Ag–O bonding.

## 2. EXPERIMENTAL

Stoichiometric amounts of reagent grade $Ag_2O$ and $B_2O_3$ were mixed and melted in Pt crucibles at 1000°C for about 30 min. Splat quenching the melts between two polished copper blocks yielded flat samples with surfaces of good quality, which were used for spectroscopic measurements without any further treatment. Clear glasses were prepared in the composition range $0 \leq x \leq 0{\cdot}33$.

Raman spectra were measured on a Ramanor HG 2S Jobin-Yvon spectrometer at 90° scattering geometry, employing the 514·5 nm line of a Spectra Physics 165 argon laser for excitation. Strong fluorescence prevented the measurement of the Raman spectra of the glasses with $x > 0{\cdot}20$. Infrared reflectance spectra were recorded on a Fourier-transform Bruker IFS 113v spectrometer in the region 30–4000 $cm^{-1}$. The absorption coefficient spectra reported in this work were calculated from the reflectivity spectra through the Kramers-Kronig inversion technique [19].

## 3. RESULTS AND DISCUSSION

### 3.1. The Structure of the Borate Network

**3.1.1. Mid-infrared spectra** - Infrared absorption spectra of silver borate glasses are presented in Fig. 1. Three spectral regions, characteristic of vibrational modes of the borate network, can be distinguished in the mid infrared part of the spectra: 1200-1550 $cm^{-1}$ (B–O stretching vibrations of trigonal $BO_3$ units), 850-1200 $cm^{-1}$ (B–O stretching vibrations of tetrahedral $BO_4$ units), and 600-800 $cm^{-1}$ (bending vibrations of various borate segments) [1,19]. The most obvious effect of the addition of $Ag_2O$ to $B_2O_3$ is the progressive development

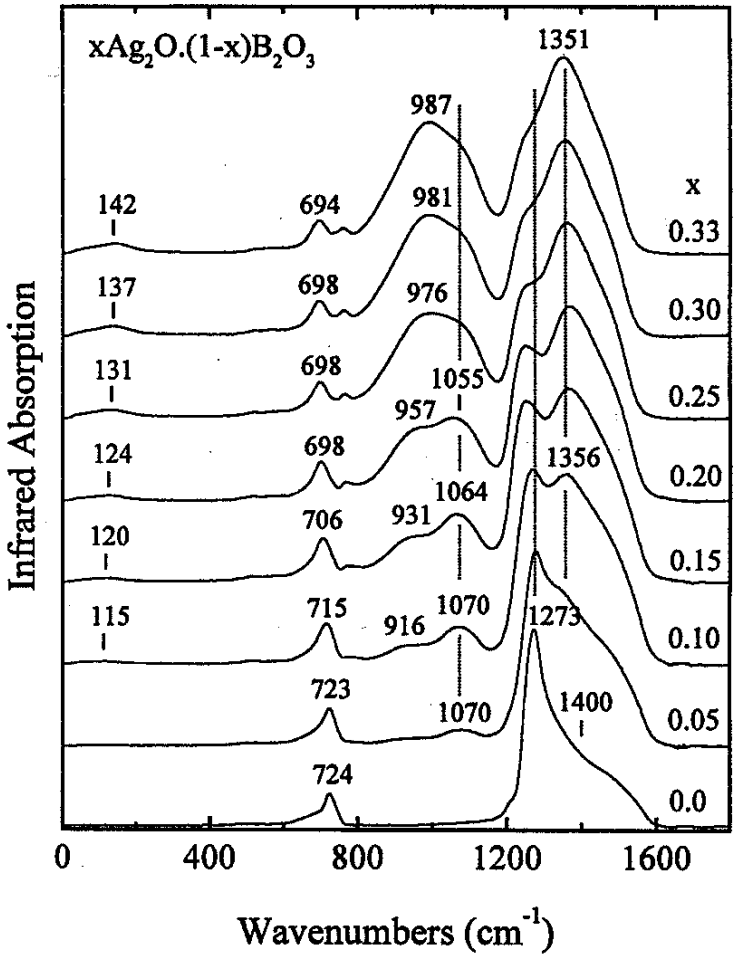


**Fig. 1.** Infrared absorption spectra of $xAg_2O.(1-x)B_2O_3$ glasses.

of a complex absorption envelope in the region 850-1200 $cm^{-1}$. Glassy $B_2O_3$ (x=0) which is known to consist of boroxol rings and independent $BO_3$ trigonal units [20] shows no infrared activity in this region. Thus, the increase of the relative intensity of the 850-1200 $cm^{-1}$ envelope with x is indicative of the progressive transformation of $BO_3$ triangles into $BO_4$ tetrahedral units. This observation suggests that $Ag_2O$ plays a role similar to that of alkali oxides, therefore confirming the network modifying nature of $Ag_2O$ suggested in previous studies [7-13].

Increasing the $Ag_2O$ content in the range $0<x\leq0{\cdot}15$ results in the appearance of two bands at *ca* 930 and 1065 $cm^{-1}$, while for higher x values a third band develops at *ca* 980 $cm^{-1}$. Comparison with the infrared spectra of alkali borate glasses and crystals suggests that the first two bands can be attributed to B–O stretching vibrations of $BO_4$ tetrahedra in pentaborate units, while the corresponding vibrations of triborate and diborate groups should be responsible for the latter feature [19]. Hence, the compositional dependence of the spectra denotes that the initially formed pentaborate units ($x\leq0{\cdot}15$) are gradually replaced by triborate and diborate groups. The presence of such borate groups, with well defined medium-range order, is in agreement with the propositions of Krogh-Moe [1] and Boulos & Kreidl [8].

The emerging structural picture is supported also by the composition dependence of the 1273 $cm^{-1}$ band, which has been attributed to the stretching

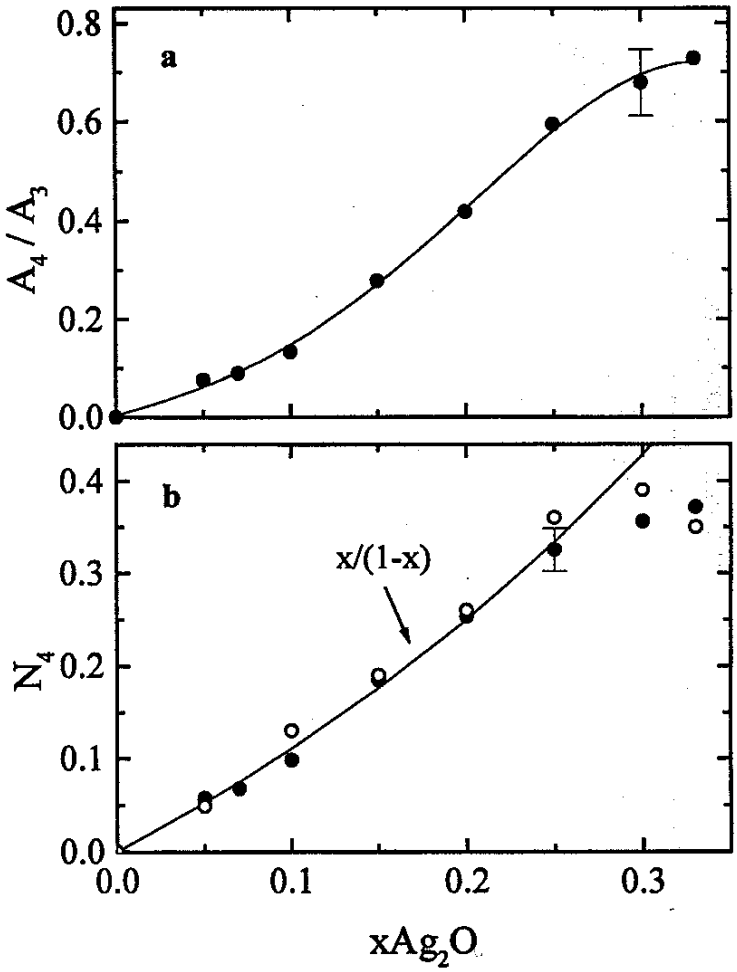


**Fig. 2. (a)** Effect of $Ag_2O$ on the relative integrated intensity $A_4/A_3$. The line is drawn to guide the eye. **(b)** The fraction $N_4$ calculated through Eq. (1) is depicted by closed symbols. The continuous line represents the theoretical $N_4=x/(1-x)$ behaviour. Open circles represent NMR data of Kim & Bray [7].

vibration of B–O–B linkages characteristic of boroxol rings, pentaborate and triborate groups [1]. The destruction of pentaborate groups in favour of diborates with increasing x is consistent also with the development of the 1351 $cm^{-1}$ feature which is characteristic of the latter arrangements [19] (x=0·33). Along the same lines is the activity exhibited by the bending vibrations: pentaborate units are active at ~710 $cm^{-1}$ and diborate ones at ~695 $cm^{-1}$ [19].

The effect of $Ag_2O$ on the short-range structure can be quantified by obtaining the integrated intensity of the absorption profiles: 800-1200 $cm^{-1}$ (denoted by $A_4$) and 1200-1550 $cm^{-1}$ (denoted by $A_3$), which are characteristic of $BO_4$ tetrahedra and $BO_3$ triangular units, respectively. The relative integrated intensity, $A_r=A_4/A_3$, was calculated and is shown in Fig. 2(a) versus $Ag_2O$ content. The change of boron coordination from three to four with increasing x is well demonstrated. As shown previously [21] the relative integrated intensity $A_r$ can be employed to calculate the fraction of four-coordinated boron atoms, $N_4$, through the expression,

$$N_4=A_r/(\alpha+A_r) \qquad (1)$$

where $\alpha$ is the relative absorption coefficient of boron tetrahedra versus boron

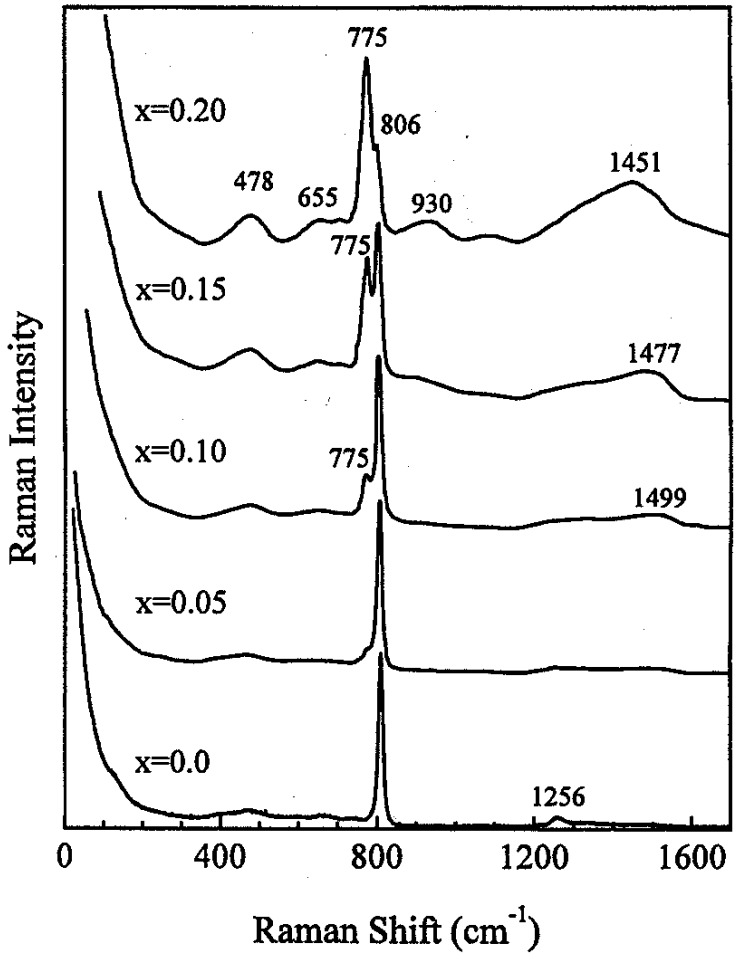


**Fig. 3.** Raman spectra of $xAg_2O.(1-x)B_2O_3$ glasses.

triangles. At very low $Ag_2O$ contents the structural modification mechanism involves mainly the transformation of boron–oxygen triangles into borate tetrahedra, and thus the law $N_4=x/(1-x)$ is obeyed. On these grounds, the experimental $A_r$ values of the x=0·05 and x=0·07 glasses and Eq.(1) give the average value $\alpha=1{\cdot}25$. With the assumption that this value of $\alpha$ is independent of x, Eq. (1) is employed to calculate $N_4$ using the infrared data ($A_r$). The results are shown in Fig. 2(b) where a comparison with the theoretical values (x/(1–x)) and the NMR results of Kim & Bray [7] is also made. It can be seen that the agreement between infrared and NMR results is good, both showing that the fraction of four-coordinated boron atoms follows the theoretical curve very closely up to $x\approx0{\cdot}25$. The deviations observed for $x\geq0{\cdot}25$ are attributed to formation of non-bridging oxygen containing metaborate triangles, $B\varnothing_2O^-$, in general agreement with the results of previous investigations [7-13].

The isomerization process $B\varnothing_4^-\Leftrightarrow B\varnothing_2O^-$ is of special importance for understanding the factors affecting the structure of alkali borate glasses below the metaborate composition, $x\leq0{\cdot}50$ [22]. High field strength cations (e.g. $Li^+$) favour the formation of $B\varnothing_4^-$, but low field strength cations (e.g. $Cs^+$) induce a higher rate of $B\varnothing_2O^-$ creation. Indeed, the $N_4$ values of Li-borate glasses follow the theoretical curve up to *ca* x=0·25, but increasing deviations were observed in the series Li<Na<K<Rb<Cs [4]. Therefore, the results depicted in Fig. 2(b) suggest that the effect of silver ions on the short-range order of bo-

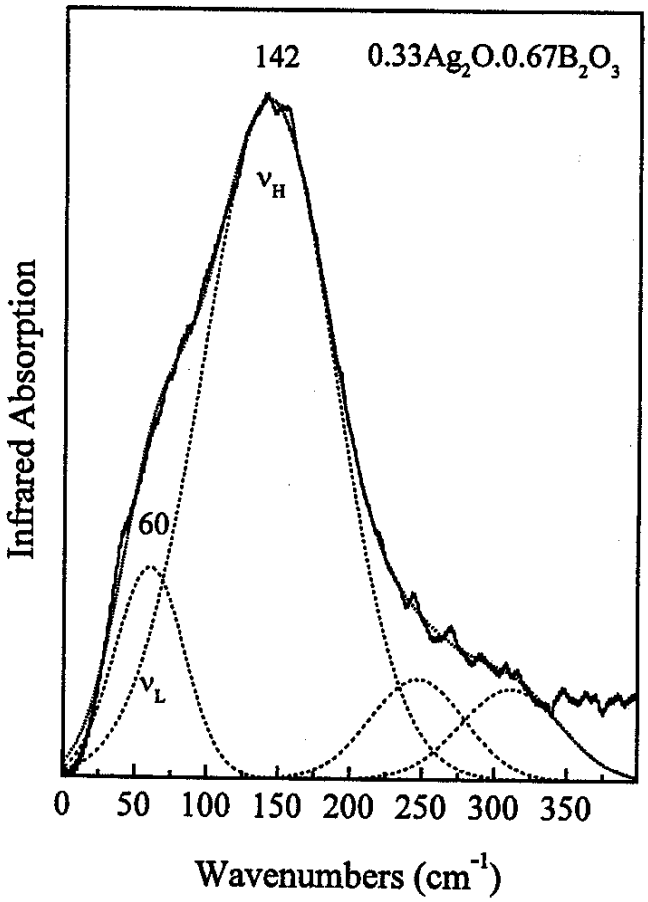


**Fig. 4.** Deconvoluted far infrared spectrum of the $0{\cdot}33Ag_2O.(1-x)B_2O_3$ glass.

rate glasses is very similar to that of lithium ions.

The change of boron coordination number from 3 to 4 enhances the coherence of the borate network because of the additional B–O–B crosslinks developed, while the formation of non-bridging oxygens results in network depolymerisation. These drastic changes of the short-range structure are manifested in the composition dependence of macroscopic glass properties, such as the glass transition temperature, $T_g$, and the thermal expansion coefficient, $\alpha$. For silver borate glasses $T_g$ shows a maximum at x=0·25, and $\alpha$ passes through a well defined minimum at x=0·20 [8,11].

**3.1.2. Raman spectra** - Figure 3 shows the Raman spectra of silver borate glasses. The spectrum of glassy $B_2O_3$ (x=0) is dominated by the sharp band at 806 $cm^{-1}$, assigned to the ring-breathing vibration of boroxol rings [23]. Addition of $Ag_2O$ causes the progressive decrease of the intensity of the boroxol band and the development of a new band at 775 $cm^{-1}$, which dominates eventually the spectrum of the x=0·20 glass. A similar band in the spectra of alkali borate glasses has been attributed to the symmetric ring-breathing vibration of six-membered rings bearing one or two $B\varnothing_4^-$ tetrahedra [22,24].

Increasing x induces changes in other regions of the Raman spectra as well. In particular, broad and asymmetric bands appear at 350-550 $cm^{-1}$, 600-700 $cm^{-1}$, 850-1000 $cm^{-1}$ and 1300-1550 $cm^{-1}$. In analogy with alkali borates, the bands at 350-550 $cm^{-1}$, *ca* 650 $cm^{-1}$ and 850-1000 $cm^{-1}$ can be attributed to the

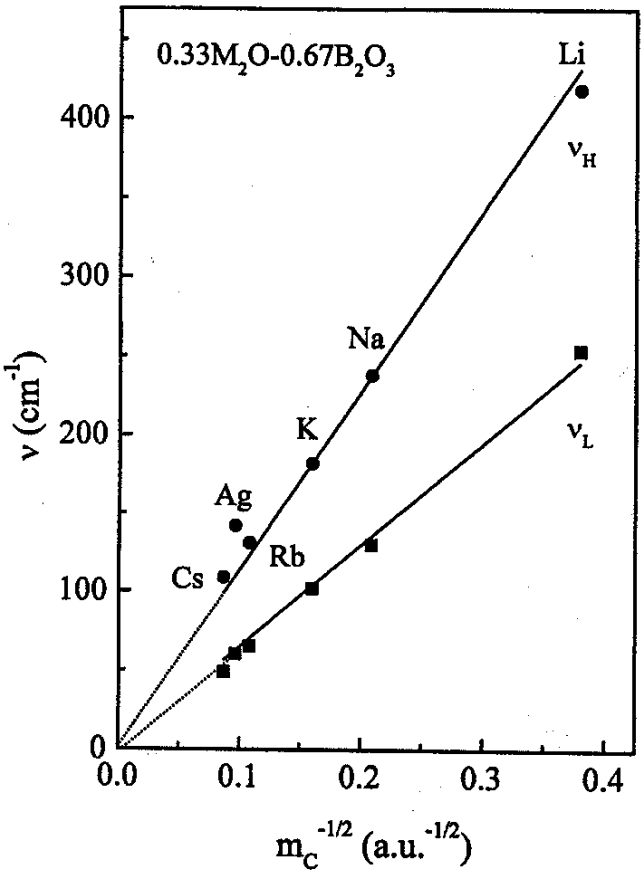


**Fig. 5.** Cation motion frequencies ($\nu_H$, $\nu_L$) versus $m_C^{-1/2}$, where $m_C$ is the metal ion mass, for silver- and alkali-diborate glasses (x=0·33). Lines are least square fittings to the alkali vibration frequencies. Error bars are of the size of symbols.

vibrations of borate tetrahedra containing borate groups, i.e. pentaborate, and triborate groups. The 1300-1550 $cm^{-1}$ band envelope changes in shape and increases in relative intensity with x. Bands in this high-frequency region have been assigned to the localised stretching vibrations of terminal B–$O^-$ bonds of metaborate triangles, $B\varnothing_2O^-$ [22]. As shown in Fig. 3, the 1300-1550 $cm^{-1}$ envelope can be observed already at x=0·10 but attains considerable relative intensity for $x \leq 0.15$, indicating an increasing rate of formation of non-bridging oxygens. At the moment, it is difficult to quantify this effect because the corresponding Raman cross section is not known. The Raman results presented in this section are in reasonable agreement with the trends observed in the corresponding infrared spectra.

### 3.2. Far Infrared Spectra and the Nature of the Ag–O Bond

The nature and distribution of anionic sites hosting $Ag^+$ ions can be revealed from the study of the far infrared spectra. It is seen in Fig. 1 that the far infrared region is characterised by the presence of a weak feature, whose intensity and frequency are increasing with $Ag_2O$ content. This band is attributed to the rattling motion of $Ag^+$ ions against their network sites [25].

A typical far infrared spectrum is shown in Fig. 4 in an expanded frequency and intensity scale. The pronounced low frequency asymmetry of the $Ag^+$ motion band can be described well by two Gaussian components, using the

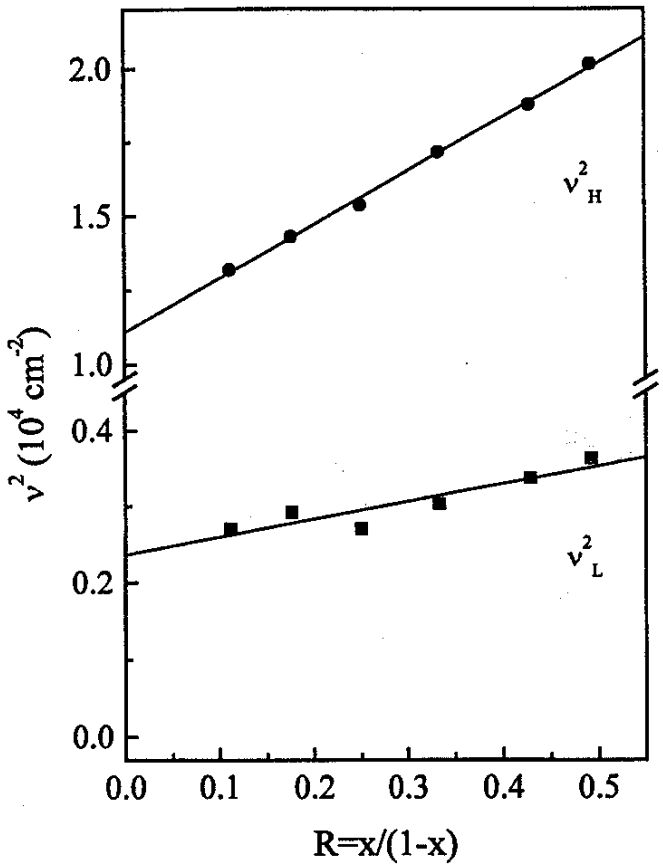


**Fig. 6.** Dependence of $\nu_H^2$ and $\nu_L^2$ on R=x/(1–x) in $xAg_2O.(1-x)B_2O_3$ glasses. The lines are least squares fittings. Error bars are of the size of symbols.

deconvolution procedure applied previously to binary and ternary glasses [19,25-27]. The two weaker components which describe absorption between 200-350 $cm^{-1}$ can be assigned to borate network modes [27]. The two far infrared components, with frequencies designated by $\nu_H$ and $\nu_L$, are attributed to vibrations of $Ag^+$ ions in two distributions of anionic site environments. It is of interest to note that the far-infrared spectra of silver borates could be described always by two Ag-ion motion components, despite the continuous variation of the short- and medium-range structure induced by $Ag_2O$ addition. The existence of two different distributions of $Ag^+$ sites can originate from the inhomogeneous dispersion of $Ag^+$ ions in the glass matrix, that may result in Ag-rich and Ag-poor regions, as suggested by Kamiya et al [15].

The $Ag^+$ motion frequencies ($\nu_H$, $\nu_L$) for the x=0·33 glass (diborate composition), and the corresponding frequencies of alkali ions in diborate glasses [27] are plotted in Fig. 5 versus $m_c^{-1/2}$, where $m_c$ is the metal ion mass. The silver motion frequencies are excluded from the linear least square fits shown in this figure. It can be seen that the $Ag^+$ ions giving rise to frequency $\nu_L$ behave as pseudo-alkalis, in contrast to those vibrating at frequency $\nu_H$. Clearly $\nu_H(Ag^+)$ is *ca* 30% higher than the $\nu_H$ frequency of an alkali-like ion with the mass of silver. The Ag- and alkali-motion frequencies in borate sites were compared for various other metal oxide contents (x) and found to exhibit trends very similar to those in Fig. 5. We interpret these results as suggesting that Ag ions vibrating with frequencies $\nu_L$ interact with their sites ionically, while those giv-

ing rise to $\nu_H$ are characterised by Ag–O bonding with considerable covalency. These findings lend support to the proposition of Tarashima and co-workers discussed in the introduction [18].

Figure 6 displays the silver ion frequencies squared ($\nu_H^2$, $\nu_L^2$) as a function of the structural parameter R= x/(1–x), which represents the average formal negative charge per boron–oxygen polyhedron. The observed linear increase of $\nu_H^2$ and $\nu_L^2$ with R can result from the creation of network sites with increasing anionic charge density, and/or from the progressive decrease of the Ag–O bond distance [28]. Both effects point to the increasing covalency in the Ag–O interactions as the content of glass in silver oxide increases.

## 4. CONCLUSIONS

The analysis of the mid-infrared and Raman spectra of silver borate glasses has demonstrated the modifying role of $Ag_2O$ on the glass structure. Thus, boroxol rings are progressively destroyed in favour of $BO_4$-containing six-membered rings, resulting in the change of boron coordination number from 3 to 4. The fraction of four-coordinated boron atoms, $N_4$, was found to follow the theoretical values, x/(1–x), for compositions in the range $0<x\leq 0{\cdot}25$. For glasses with higher silver oxide contents, both infrared and Raman spectra showed the creation of borate groups containing non-bridging oxygens.

The broad and asymmetric far infrared profiles in the range of $Ag^+$ ion motion were deconvoluted by two Gaussian bands having frequencies ($\nu_H$, $\nu_L$) and intensities which increase with x. These bands were assigned to vibrations of $Ag^+$ cations in two different distributions of network sites, suggesting the inhomogeneous dispersion of silver ions in the glass matrix. $Ag^+$ cations vibrating in their sites with frequency $\nu_H$ exhibit covalent character in their Ag–O interactions.

## REFERENCES


[1] J. Krogh-Moe, *Phys. Chem. Glasses* **6** (1965), 46.
[2] G. E. Jellison & P.J. Bray, *J. Non-Cryst. Solids* **29** (1978), 187.
[3] S. A. Feller, W. J. Dell & P.J. Bray, *J. Non-Cryst. Solids* **51** (1982), 21.
[4] J. Zhong & P.J. Bray, *J. Non-Cryst. Solids* **111** (1989), 67.
[5] E.I. Kamitsos, G.D. Chryssikos & M.A. Karakassides, *Phys. Chem. Glasses* **29** (1988), 121.
[6] G.D. Chryssikos, E.I. Kamitsos & M.A. Karakassides, *Phys. Chem. Glasses* **31** (1990), 109.
[7] K.S. Kim & P.J. Bray, *J. Non-etals* **2** (1974), 95.
[8] E.N. Boulos & N.J. Kreidl, *J. Am. Ceram. Soc.* **54** (1971), 368.
[9] G. Carini, M. Cutroni, A. Fontana, G. Mariotto & F. Rocca, *Phys. Rev. B* **29** (1984), 3567.
[10] G. Carini, M. Cutroni, M. Federico, G. Galli & G. Tripodo, *Phys. Rev. B* **30** (1984), 7219.
[11] J.L. Piguet & J.E. Shelby, *J. Am. Ceram. Soc.* **68** (1985), 450.
[12] G. Dalba, P. Fornasini, F. Rocca, E. Bernieri, E. Burattini & S. Mobilio, *J. Non-Cryst. Solids* **91** (1987), 153.
[13] J. Swenson, L. Börjesson & W.S. Howells, *Phys. Rev. B* **52** (1995), 9310.
[14] G. Chiodelli, G. Campari Vigano, G. Flor, A. Magistris & M. Villa, *Solid State Ionics* **8** (1983), 311.
[15] K. Kamiya, S. Sakka, K. Matusita & Y. Yoshinaga, *J. Non-Cryst. Solids* **38&39** (1980), 147.
[16] M.C. Abramo, G. Carini & G. Pizzimenti, *J. Phys. C: Solid State Phys.* **21** (1988), 527.
[17] M.C. Abramo, G. Pizzimenti & G. Carini, *Solid State Ionics* **28-30** (1988), 148.

[18] K. Tarashima, S.H. Kim & T. Yoko, *J. Am. Ceram. Soc.* **78** (1995), 1601.
[19] E.I. Kamitsos, A.P. Patsis & G.D. Chryssikos, *J. Non-Cryst. Solids* **126** (1990), 52.
[20] A.C. Hannon, R.N. Sinclair, J.A. Blackman, A.C. Wright & F.L. Galeener, *J. Non-Cryst. Solids* **106** (1988), 116.
[21] G.D. Chryssikos, J.A. Kapoutsis, E.I. Kamitsos, A.P. Patsis & A.J. Pappin, *J. Non-Cryst. Solids* **167** (1994), 92.
[22] E.I. Kamitsos & G.D. Chryssikos, *J. Mol. Struct.* **247** (1991), 1.
[23] C.F. Windisch & W.M. Risen Jr., *J. Non-Cryst. Solids* **48** (1982), 281.
[24] T.W. Brill, *Phillips Res. Rep., Suppl.* No. **1** (1975), 1.
[25] E.I. Kamitsos, J.A. Kapoutsis, G.D. Chryssikos, J.M. Hutchinson, A.J. Pappin, M.D. Ingram & J.A. Duffy, *Phys. Chem. Glasses* **36** (1995), 141.
[26] J.A. Kapoutsis, E.I. Kamitsos, G.D. Chryssikos, Y.D. Yiannopoulos, A.P. Patsis & M. Prassas, *Chim. Chron. New Series* **23** (1994), 271.
[27] E.I. Kamitsos, A.P. Patsis & G.D. Chryssikos, *J. Non-Cryst. Solids* **152** (1993), 246.
[28] E.I. Kamitsos, G.D. Chryssikos, A.P. Patsis & J. A. Duffy, *J. Non-Cryst. Solids* **196** (1996), 249.